Online Action Learning using Kernel Density Estimation for Quick Discovery of Good Parameters for Peg-in-Hole Insertion

Lars Carøe Sørensen, Jacob Pørksen Buch, Henrik Gordon Petersen and Dirk Kraft
SDURobotics, The Maersk Mc-Kinney Moller Institute, University of Southern Denmark, Campusvej 55, Odense, Denmark

Keywords: Learning and Adaptive Systems, Compliant Assembly, Intelligent and Flexible Manufacturing.

Abstract: Learning action parameters is becoming an ever more important topic in industrial assembly with tendencies towards smaller batch sizes, more required flexibility and process uncertainties. This paper presents a statistical online learning method capable of handling these issues. The method uses elimination of unpromising parameter sets to reduce the elements of the discretised sample space (inspired by Action Elimination) based on regression uncertainty. Kernel Density Estimation and Wilson Score are explored as internal representations. Based on a dynamic simulator setup for a real world Peg-in-Hole problem, it is shown that the presented method can drastically reduce the number of samples needed. Furthermore, it is also shown that the solution obtained in simulation by our learning method succeeds when executed on the corresponding real world setup.

1 INTRODUCTION

Introducing industrial robot arms into assembly batch productions with low volume and high variance (both part variations and process uncertainties), has caught an increasing interest recently (EU Robotics aisbl, 2014; Robotics VO, 2013). Classically, part variations and process uncertainties in assembly production are addressed by designing highly specialised equipment (e.g. engineered gripper fingers or feeder systems), which is time-consuming, expensive in construction, and inflexible when changing process. Since few-of-a-kind productions entail frequent process changes due to the low batch volumes, it is at the moment often cost prohibitive to introduce robots in this field. To overcome these challenges, high flexibility is very important. Flexibility is obtainable by being able to inexpensively shift between different assembly processes with low setup times. An example of a process which is challenged by unhandled part variations and process uncertainties is the tight fitting Peg-in-Hole (PiH) process (see Figure 1). Parameters in such a process are very hard to tune by hand since the selected solution is not guaranteed to succeed every time. We address this problem by a robust optimisation of PiH action parameters in simulation. Another possible approach would be to introduce sensor-controlled actions, but these typically slows the process down and increases complexity and system cost.

In previous work (Buch et al., 2014), a framework for accomplishing these assembly batch productions was introduced. It was shown how an assembly process can be parametrised.

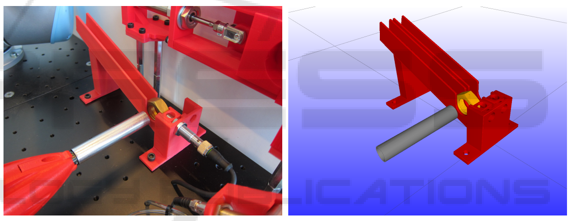
Figure 1: The real test setup of the addressed PiH case (left) and the corresponding dynamic 3D simulation used for parameter optimisation (right).

The sample spaces of these types of assembly processes are often large due to the number of parameters and their ranges. This problem becomes even more severe when including part variations and process uncertainties since several examinations of each sample point are necessary to determine the underlying success probability. Therefore, a method capable of handling action parameter optimisation by a fast reduction of these large parameter spaces is needed to sort out uninteresting regions of the sample space.

This paper presents a global iterative learning method for optimisation of processes where part variations and process uncertainties highly influence the result. The method uses both an estimate of the true success probability and an uncertainty measure to find suitable sets of action parameters. Part variations

Sørensen, L., Buch, J., Petersen, H. and Kraft, D.
Online Action Learning using Kernel Density Estimation for Quick Discovery of Good Parameters for Peg-in-Hole Insertion.
DOI: 10.5220/0005958801660177
In *Proceedings of the 13th International Conference on Informatics in Control, Automation and Robotics (ICINCO 2016) - Volume 2*, pages 166-177
ISBN: 978-989-758-198-4

and process uncertainties are taken into account by the uncertainty measure in the learning method while searching the parameter space for a successful and robust solution. The iterative learning method adapts to regions of the parameter space where good parameter sets can be found. This adaptation is obtained by excluding bad regions in the parameters space with probabilistic certainty. The intention of the presented iterative learning method is to focus on achieving sufficient knowledge about all promising regions and thereby reduce the total number of simulations needed. This approach can be compared to traditional Reinforcement Learning (RL) methods where the aim is only to reduces the number of failures (also referred to as the regret, see e.g., (Auer et al., 2002)). Moreover, the dynamic simulation of actions is seen as rather time-consuming, and is therefore characterised as being an expensive cost function. This is also one of the main reasons for minimising the total number of simulations needed, since this reduces the setup time. Some approaches do not consider the computation-time of the "learning part" between executions where the next parameter set is selected since only the number of executions are of concern. However, for us this is not a possibility since the goal is to minimise the total setup time. While we do in this paper only analyse the number of simulations and not the computation time of the learning, this is still an important aspect.

Since our iterative learning method relies on a suitable estimate of the true success probability and the uncertainty measure, we investigate possible data representations for these two values. We show that by taking experiments made in the neighbourhood into account, it is possible to reduce the number of simulations needed to find promising regions with high success probability of the parameter space. We compare our results to both the simple Naïve Sampling (NS) and to Wilson Score (WS) that does not consider the value of neighbouring samples. We model the influence of the neighbourhood by Kernel Density Estimation (KDE), where the smoothing effect of the kernel assumes correlation within the neighbourhood region. We apply the above concept to a tight fitting (also known as low clearance fit or restrictive tolerance) PiH process for which good parameter sets are found by dynamic simulation and verified on a real test setup (see Figure 1).

We start by presenting work related to our method in Section 2. In Section 3 we first discuss different data representations concerning estimation of the true success probability and the corresponding uncertainty measure used by the iterative learning method. This section also describes how a kernel size for the KDE can be obtained. Afterwards Section 4 describes the general approach of the iterative learning method and how the adaptive behaviour is obtained by elimination. In Section 5 the necessary preparation for the experiments is described. In Section 6 experiments with the iterative learning method are carried out along with a discussion of the results obtained. Lastly, Section 7 summarises on the outcome of the project.

2 RELATED WORK

The PiH problem, and learning strategies to solve it, has been investigated in many aspects over the past decades. Recent results include for example (Li et al., 2014; Yang et al., 2015; Bodenhagen et al., 2014). We will in the following point out different important aspects, while also mentioning some applied approaches.

The general problem of learning action parameters is of great concern in robotics also beyond PiH and has many sub-aspects. We will here focus mostly on works related to our approach and will therefore not discuss in detail approaches that make use of execution feedback beyond a binary result in the learning process (e.g., a vector representing error forces during insertion used as gradient to update the actions) nor methods that use sensorial feedback during execution (see e.g., (Yang et al., 2015; Gams et al., 2014)). Furthermore, we will also limit our discussion on how to represent actions (see e.g., (Ijspeert et al., 2012) for the popular DMP representation, (Bodenhagen et al., 2014) using splines for PiH or (Detry et al., 2011) using 6D poses) but just assume that we have an action representation that has a set of parameters.

Optimisation criteria for learning manipulation actions can be diverse, examples include execution time, final system state (e.g., is the flexible object placed as flat as possible) and a very straight forward high success probability, which is the criteria used in our work.

The last important aspect to discuss is learning approaches. We will, therefore in the following, describe a set of learning approaches that can be applied to problems of the form discussed up till now.

Policy Search methods look directly for good parameters in a given policy parametrisation. In comparison to classical Reinforcement Learning (Sutton and Barto, 1998), policy search is independent of the value function and the state-action relationship, but only depends on the rewards received after completing a full execution with a fixed policy. The policy is then iteratively updated to maximise the reward outcome during several executions (Deisenroth et al., 2011). A good policy parametrisation limits the search space of possible policies and can thereby reduce the learning-costs. The general approach for learning good policies are by local methods such as gradient descent (e.g., (Williams, 1992)) and evolutionary methods (e.g., (Heidrich-Meisner and Igel, 2009)). These methods are often preferred in robotics, since they locally adapt the given policy, and thereby avoid trying a very different policy which may destroy the robot setup. Compared to global methods (e.g., the one presented in this work) these local methods need a good starting point and only find one local optimum. Since we seek the overall highest success probability, global methods are preferable. Moreover, global methods are also capable of finding multiple global optimums. This is useful in situations where the currently select solution becomes unusable (e.g. unreachable).

Kernel Density Estimation (KDE) (Silverman, 1986) has become a popular technique for a wide range of applications and methods (Bodenhagen et al., 2014; Detry et al., 2011) to estimate success probabilities. KDE is typically used to represent successful action parameters. In (Detry et al., 2011) KDE is used to express the link between object grasp poses and their corresponding success density to learning suitable stable grasps of objects. The method takes advantage of kernel smoothing done by KDE to utilise the likely fact that two close lying parameter sets have nearly the same success probability. KDE can also be used to obtain the success probability as in (Bodenhagen et al., 2014), where also failures are taken into account. We will use this approach to represent the success probability of action parameters.

Bayesian Optimisation (BO) aims at minimising the number of function evaluations while searching the sample space for the optimal solution (Brochu et al., 2010). In BO, an estimate of the underlying function is used to form an acquisition function from which a maximisation process selects the next sample to investigate. Often Gaussian Processes (GP) are used as the function estimate from which a trade-off between the GP mean and variance defines the acquisition function. This approach has been used in (Tesch et al., 2013) where the GP estimate has been transformed to fit with stochastic binary outcomes. In (Park et al., 2014) Gaussian Processes and K-Nearest Neighbour are used to estimate the probability for a successful solution when reaching for objects in highly cluttered environments with mobile robots. Such environments differ from our field of interest by being very unstructured. Our environments are structured, but part variations and process uncertainties need to be taken into account during the optimisation to obtain useful and robust solutions, which is not actively incorporated in the approach of (Park et al., 2014). Our approach mostly differs from GP in the estimation of the underlying function. The GP variance expresses the density of samples (a dense sampling results in low variance and vice versa), where in our implementation of KDE the variance expresses the data uncertainty, which helps in obtaining a robust final result.

To cope with large parameter spaces we use *elimination*[1], where sub-optimal solutions are eliminated during the learning process. This approach reduces the search space by eliminating certain bad solutions discovered and the focus is therefore only on the promising points. In (Even-Dar et al., 2006) several different elimination algorithms are presented such as the Successive and Median Elimination and the Model-Based Elimination (MBE). Instead of selecting the parameter set with highest upper bound as IE, the MBE eliminates a parameter set from further selection if its confidence interval does not overlap with the current best. This approach is similar to ours, but instead of permanently eliminating a parameter set, we allow it to be reconsidered, if the surrounding neighbourhood suggests so through the KDE probability estimate.

In (Jørgensen et al., 2016) several optimisation methods are investigated, where the solutions are post-evaluated by a robustness measure. This approach differs from ours by not including the part variations and process uncertainties when searching for the solutions, but only during the evaluation.

Our method is first of all characterised by being a global and online approach for learning parameters robust to part variations and process uncertainties. Moreover, elimination is used to exclude certain bad areas of the sample space. The regression estimate and the uncertainty measure used by the elimination is obtained through Kernel Density Estimation.

3 THE INTERNAL DATA REPRESENTATIONS

It is preferable to describe internal data representations before explaining the approach of our iterative learning method in details. The reason is that these representations define how the estimated regression and the associated uncertainty measure are obtained, which is used by the learning method when exclud-

[1]We use the term elimination here for what is known in the literature as *Action Elimination* to avoid confusion with our definition of an Action.

ing bad sample points and afterwards selecting the next sample for investigation. Moreover, the choice of representation highly impacts the performance of the iterative learning method. In this work, we only consider representations that can deal with binomial values due to the binary outcome of the experiments.

In statistics, the confidence interval is often used to describe the variance in experiment outcomes, which in this work describes the uncertainty of the sample point value. In general, the confidence interval around the regression estimate is expressed as:

$$\hat{\mu} \pm um \tag{1}$$

where $\hat{\mu}$ is the regression estimate of the true mean μ and *um* is the uncertainty measure.

The possible data representations can be split into two groups. The first group consists of *neighbourhood independent representations*, where all sample points are treated independently without any influence from the value of the surrounding samples. The second group consists of *neighbourhood dependent representations*, where a particular point is influenced by the value of the surrounding sample points.

Before explaining the neighbourhood independent and dependent representations, it is necessary to define several terms.

3.1 Definitions

We define a set of action parameters X in the parameter space S as $X \in S$. Moreover, the execution of an action with a parameter set X results in a binary outcome O. For the general notation, X and O are both random variables. From these definitions, it follows that the evaluation of the i-th experiment taken in the parameter space S is described by a two-tuple (x_i, o_i), where x_i specifies a specific parameter set and o_i is the associated outcome of the experiment. Since the outcome is defined as binomial it either results in a success s or failure f, hence $O \in \{s, f\}$.

After the evaluation of the experiment, the outcome is used to update the regression estimate and uncertainty measure. The updated information can then be used in subsequent iterations to refine the selection of the next parameter set to investigate. In the remainder of this work, we will also refer to a specific set of action parameters as a sample in S.

3.2 Neighbourhood Independent Data Representation

The first data representation evaluated for our learning scheme is the Wilson Score (WS) mean and confidence interval for binomial values (Agresti and Coull, 1998), which is a neighbourhood independent representation. Compared to the widely used Normal Approximation (NA) estimate (Ross, 2009), WS gives a usable estimate of the mean and an associated confidence interval when only few samples exist for a particular point. WS handles this by adjusting the NA mean to around 0.5 due to the lack of knowledge when having a low number of samples, but also by correcting the confidence interval to cope with NA mean at the extremes (close to zero or one).

The NA mean which is included in the calculation of the WS mean and uncertainty measure is given by:

$$\hat{\mu}_{na} = \frac{1}{n_j} \sum_{i=1}^{n_j} o_{ij} \tag{2}$$

where o_{ij} is the outcome of the i-th experiment in the j-th sample point and n_j is the total number of experiments in this particular sample point.

The WS estimated mean is expressed as:

$$\hat{\mu}_{ws} = \frac{\hat{\mu}_{na} + \frac{1}{2n_j} z^2}{1 + \frac{1}{n_j} z^2} \tag{3}$$

where z is the (1-$\alpha/2$)-quantile of a standard normal distribution (α is predefined to e.g. a 95% confidence interval).

The uncertainty measure around the WS mean is given by:

$$um_{ws} = \frac{1}{1 + \frac{1}{n_j} z^2} \cdot z \sqrt{\frac{1}{n_j} \hat{\mu}_{na}(1 - \hat{\mu}_{na}) + \frac{z^2}{4n_j^2}} \tag{4}$$

The confidence interval by WS is obtainable through the regression estimate and uncertainty measure given by (3) and (4) respectively. It should be mentioned that both the mean and uncertainty measure of WS and NA become asymptotically equivalent when the number of samples grows ($n_j \to \infty$).

3.3 Neighbourhood Dependent Data Representation

This section first explains how a regression estimate by KDE is obtained and then how to find the size of the kernel.

3.3.1 Regression Estimate and Uncertainty Measure by Kernel Density Estimation

The second representation evaluated is non-parametric KDE which provides both a neighbourhood dependent estimate on the regression value and an associated uncertainty measure. Using KDE and Bayes' Rule a regression estimate is obtained along with a pointwise confidence interval around the KDE regression (Härdle et al., 2004).

The kernel based approach of KDE tries to model the underlying function by taking advantage of kernel smoothing. However, note that KDE suffers from the typical drawbacks of smoothing techniques, i.e. the removal of detail.

The estimate of the true probability density function $p(x)$ has to be defined by KDE, see (Härdle et al., 2004), before a regression estimate and uncertainty measure can be obtained:

$$\hat{p}_H(x) = \frac{1}{n}\sum_{i=1}^{n} K_{H,x_i}(x) \tag{5}$$

where K is a user defined kernel with the bandwidth matrix H placed at x_i describing the correlation between every parameter set x and the parameter set for the i-th sample. Moreover, n is the total number of samples for the whole parameter space.

An estimate of the true regression can by KDE be expressed as (Härdle et al., 2004):

$$\hat{\mu}_H(x) = \frac{\hat{p}_O(x,s)}{\hat{p}_X(x)} = \frac{n^{-1}\sum_{i=1}^{n} K_{H,x_i}(x) O_i}{n^{-1}\sum_{j=1}^{n} K_{H,x_j}(x)} \tag{6}$$

The estimate $\hat{p}_O(x,s)$ is expressed in general terms by weighting each kernel with the outcome of the individual samples. By defining the binomial outcome of an experiment as $O \in \{s, f\} = \{1, 0\}$, then $\hat{p}_O(x,s)$ becomes a sum of only the successful samples divided by n. The estimate $\hat{p}_X(x)$ is equivalent to (5) where all samples are included no matter the outcome. Equation (6) can be expressed in more compact form as:

$$\hat{\mu}_H(x) = \frac{1}{n}\sum_{i=1}^{n} W_{H,i}(x) O_i \tag{7}$$

It is possible to derive an approximation of the asymptotic pointwise confidence interval around the regression of (7) (Härdle et al., 2004). The uncertainty measure can be calculated as:

$$um_H = z \cdot \sqrt{\frac{||K||_2^2 \; \hat{\sigma}_H^2(x)}{n \; |H| \; \hat{\mu}_H(x)}} \tag{8}$$

where $|H|$ is the determinant of H, z is again the (1-$\alpha/2$)-quantile of a one-dimensional standard normal distribution and $||K||_2^2$ the squared L_2 norm of the standard normal kernel obtained by having an identity co-variance matrix ($\int \{K(u)\}^2 du$). It should be noted that the estimated regression is a one-dimensional predictor variable and the associated confidence interval is also a scalar. The variance estimate $\hat{\sigma}_H^2(x)$ is given by:

$$\hat{\sigma}_H^2(x) = \frac{1}{n}\sum_{i=1}^{n} W_{H,i}(x)\Big(O_i - \hat{\mu}_H(x)\Big)^2 \tag{9}$$

The confidence interval by KDE is obtainable through the regression estimate and uncertainty measure given by (6) and (8) respectively.

3.3.2 Finding the Optimal Kernel Size for KDE

Before applying KDE, a suitable bandwidth matrix has to be found. We define the optimal bandwidth matrix as the one that minimises the error between the true function $\mu(x)$ and the estimated function $\hat{\mu}_H(x)$ and thereby making the optimal smoothing over the entire space, S.

A convenient global error function for the KDE regression is the Absolute Squared Error, ASE. However, ASE is not usable when the true function $\mu(x)$, is unknown. An approximation of ASE that only uses the known data can be found using the Cross-Validation (CV) principle (Härdle et al., 2004):

$$CV(H) = \frac{1}{n}\sum_{i=1}^{n}\Big(\hat{\mu}_{H,-i}(x_i) - o_i\Big)^2 \tag{10}$$

where $\hat{\mu}_{H,-i}(x_i)$ is the leave-one-out estimator which is identical to $\hat{\mu}_H(x_i)$ in (6) except that it omits the i-th experiment in both numerator and denominator. Also here n is the total number of samples for the whole parameter space.

4 THE ITERATIVE LEARNING METHOD

Problems caused by part variations and process uncertainties often only arise during certain stages of the assembly process. In our approach, each of these stages is individually handled and parametrised into an *action* for which optimal parameters are found through simulation. For the tight fitting Peg-in-Hole operation, part variations and process uncertainties highly impact the insertion of the peg into the hole and thereby the overall success probability of the process.

Since an action is a stochastic process, multiple executions of a certain parameter set are generally necessary to reveal the true success probability. To include the uncertainty on the estimated regression value in the presented method, a sample point in S is therefore described by an estimated *regression value* of the success probability, but also an *uncertainty measure* expressing the certainty bounds of the regression value.

The goal is then to find a set of parameters that leads to a high success rate (regression value) and thereby is robust to part variations and process uncertainties (e.g. initial placement of parts in the scene).

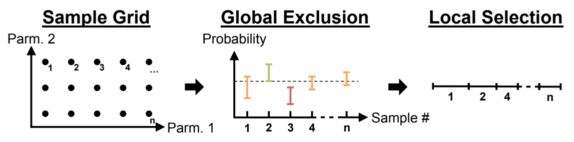

Figure 2: The learning mode with example values.

Furthermore, it is necessary to sufficiently cover the parameter space. However, the number of dimensions (parameters) and their ranges makes uniform sampling infeasible due to the large number of experiments that would be needed. This can be handled by adapting to regions with a certain high success probability and thereby avoid making unnecessary evaluations of bad regions. This results in a trade-off between obtaining a reasonable amount of knowledge distributed over the entire parameter space (exploration) and focussing attention on possible good regions (exploitation). The iterative learning method presented here uses elimination to steer its focus into regions which potentially have a high success probability. Moreover, it is possible to have multiple sets of promising parameters which might be distributed in different regions of the parameter space.

4.1 The Learning Mode

The learning method described in this work is based on a simple three-step iterative reward-based approach by first selecting a parameter set, then executing the action with these parameters which results in a success or failure outcome, and lastly use this outcome subsequently to update estimates used for the next selection.

The selection of the next parameter set to investigate would, in classic RL, be either random or greedy (choosing the best sample so far). We aim for a guided exploration strategy.

To make this selection easy to handle, we discretise the parameter space. This is done by individually making a uniform division of each parameter. By a discretisation, the learning method is restricted to only carry out experiments in these predefined points (see left part of Figure 2), which ensures that the entire space S is fully covered.

In the learning mode, we want to increase the confidence about promising samples regression values based on the current knowledge. This is done in two parts: first a global exclusion and afterwards a local selection.

In the *global exclusion* (see middle part of Figure 2) unpromising samples are excluded by elimination (Even-Dar et al., 2006). If the confidence interval of the best sample (highest estimated regression value) and a sample under consideration does not overlap then the sample is excluded.

In the second part of the learning mode a *local selection* is made (see right part of Figure 2), where one of the samples remaining after the global exclusion is selected for investigation. A sample is chosen at random based on the size of the confidence intervals, such that samples with a high uncertainty measure (large confidence interval) have a higher chance of being selected. This weighted selection is made to reduce uncertainty in the promising regions and thereby increase the overall knowledge among the remaining samples.

Global exclusion and local selection in the learning mode together ensure that only promising samples are investigated further and that the uncertainty among these good candidates is reduced.

5 EXPERIMENTAL SETUP

This section describes the experiment setup. We start by introducing our Peg-in-Hole process and by defining parameters for optimisation in Section 5.1. In Section 5.2 the use of the dynamic simulator is explained, and in Section 5.3 several implementation choices are discussed.

The real world test setup (see also Figure 1) consists of a UR5 robot arm with an attached two-fingered gripper (Robotiq Adaptive Gripper, C-Model). Even though the workpieces are placed in fixtures, the process still has part variations e.g. imperfect shape of the peg; and process uncertainties e.g. the exact placements of the workpieces. We use a real industrial assembly PiH process as test case where a metal pipe is inserted into a brass fitting. The difference in radius between the pipe (the peg) and the hole in the brass fitting is less than $0.5\,mm$. A simple linear insertion of the peg into the hole has a too high failure rate due to the tight fitting PiH process.

5.1 The Peg-in-Hole Action, Parameters and Ranges

The PiH action is broken down into three movements defined by four parameters, as shown on Figure 3. These four parameters do, with boundaries, define the search space S.

To describe our PiH action, ideal movements (without part variations and process uncertainties added to the workpieces) are assumed. In the PiH action, the peg starts at an angle θ. In the first movement the peg is moved towards the hole in a straight line with an angle φ, and this movement ends when

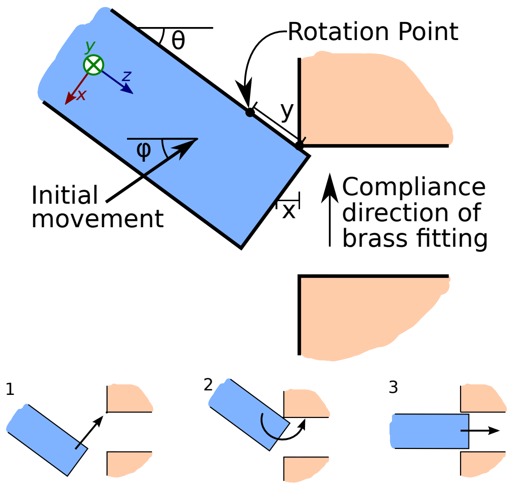

Figure 3: The PiH action. *Top:* The four parameters defining the PiH parameters. *Bottom:* The three movements of the PiH action as defined by the four parameters.

the peg touches the hole. The location of the peg at this point is defined by the perpendicular distance x from the hole to the centre of the end of the peg. Secondly, a circular movement of the peg is made around the "Rotation Point" defined by the parameter y. This movement ends when the peg is perpendicular to the surface of the hole. The last movement is a linear insertion of the peg into the hole.

From the above description, the ideal relative path between the peg and hole is calculated for the chosen parameter set. This path can then be executed in simulation and on the real world setup under the influence of part variations and process uncertainties.

It is considered a success if the peg is placed into the hole after the execution ends; otherwise a failure (e.g. if the peg gets stuck by hitting the brass fitting). This evaluation is automatically labelled in simulation but manually done for real world experiments.

Compliance between peg and hole is an important factor to prevent high contact forces which can damage both robot, equipment and item when not having sensorial feedback. This compliance is utilised under the circular movement to overcome the part variations and process uncertainties. In the test case, compliance is present by letting the brass fitting move upwards in the feeder system following the direction of compliance (see Figure 3).

The ranges of the parameters are chosen in advance of the experiment and define the boundaries inside which the iterative learning method can perform the search. In this work, we will limit ourselves to the investigation of the three parameters x, θ and φ, while fixing the fourth parameters y to $10\,mm$. The ranges of the parameters are manually chosen to $[-5;5]\,mm$, $[0;30]^{\circ}$ and $[0;45]^{\circ}$ for x, θ and φ respectively based on prior knowledge of the test case. The limitation to three parameters makes visualisation and inspection easier to handle and decreases the computation time. The method is not limited to three or fewer parameters in general, but the subject of dimensional scaling has to be further investigated.

5.2 The Dynamic Simulator

The quantity of experiments needed for a reliable estimation often makes it infeasible to use real world experiments. In addition, simulations are typically easier to setup (given a usable framework) and can provide automatic process evaluation, which is often difficult in the real world. Therefore, we use simulation as a tool for finding good parameters in this work.

The choice of simulator engine relies on its ability to make realistic dynamic simulations in high quantities. AnonymousEngine (Thulesen and Petersen, 2016) is such a simulator.

To make it possible for the iterative learning method to deal with part variations and process uncertainties, corresponding perturbations are added to the relevant workpieces for each simulation. Note that the simulator itself is deterministic, but the learning method does see a non-deterministic process due to the added perturbations.

Each perturbation is drawn from a predefined density distribution reflecting the part variations and process uncertainty in the real assembly process. In our PiH test case translational perturbations are made independently along the x- and y-axis of the peg (see Figure 3), both drawn from a normal distribution with standard deviation of $0.35\,mm$, where the confidence level is chosen to 95% ($z = 1.96$). If this value exceeds plus/minus one standard deviation a new draw is made since extreme values do not occur in the real world PiH test case. This results in a maximum translation of $\pm 0.49\,mm$.

5.3 Experiment Choices

In this section we select first the type of kernel, then the bandwidth matrix used by the KDE representation is found, and lastly a discretisation of the parameter space is made.

5.3.1 The Kernel Type and Bandwidth

In this work we choose to use a diagonal multinormal (Gaussian) kernel to reduce complexity when the optimal bandwidth has to be found. This choice does assume independence between the parameters but leaves only three elements (one for each of chosen parameters) for which the optimal values should be found instead of six elements when using a full bandwidth matrix. Note that the matrix must be symmetric and positive definite.

The bandwidth matrix used in the case is transferred from a previous similar case. We do believe that a suitable kernel size can be transferred from similar cases. This means that simulations made for optimising the kernel are reused and omitted when setting up a similar case.

The Cross-Validation (CV) error function was used (see Section 3.3.2) to find a suitable bandwidth matrix in the previous case. The error function was minimised using the Coordinate Descent algorithm to find the optimal bandwidth matrix, H. The samples were drawn randomly from a uniform distribution over the entire parameter space, S. The minimisation was performed five times and each time with 5000 randomly chosen samples. This was done to account for both the stochastic behaviour of the process and to ensure sufficient coverage of the parameter space. The average of the five minimisations equates to:

$$H = diag\left(h_x = 0.20\,,\, h_\theta = 0.93\,,\, h_\varphi = 8.18\right) \quad (11)$$

5.3.2 Discretisation of the Parameter Space

To have a discretisation which both covers the space and where the chosen kernel can influence neighbourhood points, it was decided to have 1.5 standard deviations between each of sample points. Based on (11) and the parameter ranges this leaves a discretisation of 35, 23 and 5 steps for the three parameters x, θ and φ respectively, which results in a grid consisting of 4025 sample points.

6 EXPERIMENTS AND RESULTS

This section shows how the iterative learning method can be used to find promising parameter sets by fast reduction of the parameter space. Section 6.1 compares the performance of the iterative learning method using Kernel Density Estimation with Wilson Score and simple Naïve Sampling. In Section 6.2 a promising parameter set found by the learning method with KDE is tested on a real world setup.

6.1 Applying the Iterative Learning Method

In this section, we first apply the iterative learning method with WS and find that the number of samples

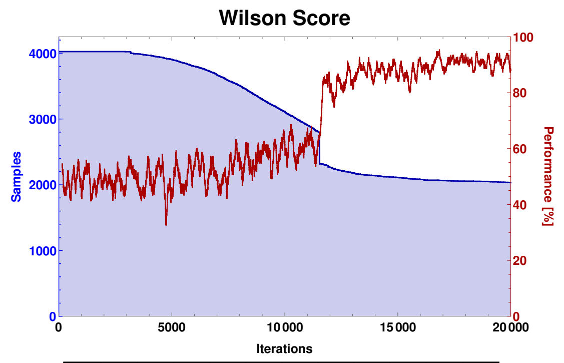

Ite.	1	2000	4000	6000	8000	10k	12k	14k	16k	18k	20k
Samp.	4025	4025	3967	3801	3508	3108	2267	2139	2082	2055	2033

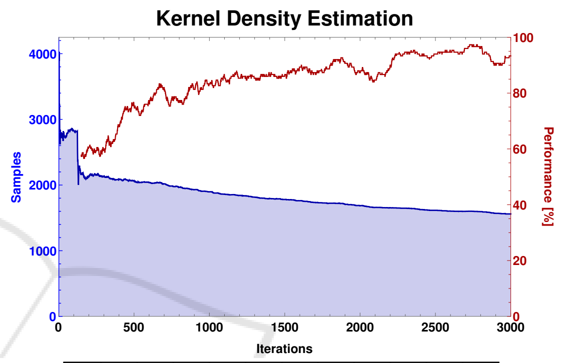

Ite.	1	300	600	900	1200	1500	1800	2100	2400	2700	3000
Samp.	4025	2135	2039	1929	1842	1780	1723	1659	1626	1599	1560

Figure 4: *Blue graph:* The number of samples still in consideration after global exclusion when applying the iterative learning method. *Red graph:* The performance of the learning method by the percentage of successful experiments within the past 150 iterations. The table below show the number of samples of samples still in consideration at the given iteration. *Top:* using WS representation for 20.000 iterations. *Bottom:* using KDE representation for 3000 iterations. Note the different scales of the horizontal axes.

needed is high compared to KDE where the neighbour samples are taken into account. Afterwards, we study the performance of the KDE estimate by comparing the obtained regression values with a simple NS. Lastly, a set of action parameters is chosen for the real world experiment.

6.1.1 Comparison Between the WS and KDE Data Representations

A comparison between WS and KDE is shown in Figure 4. The blue plot and the table below each graph expresses the number of sample points still in consideration after the global exclusion by the iterative learning method. The red graph shows the performance of the learning method by the percentage of successful experiments within the last 150 iterations.

For WS, the number of samples slowly decreases during the iterations. The large exclusion of 470 samples after 11541 iterations occurs since these samples suddenly do not overlap with the current best sample. Afterwards, the decrease in the number of samples still in consideration levels off. This shows that a large number of iterations are used for exploring the parameter space in the beginning, after which the focus is turned towards the most promising samples in the parameter space. Compared to the WS results it is clear that KDE quickly excludes what is believed to be the bad regions of the sample space, and hereafter only spends time refining the knowledge in the more promising region with further exclusions.

From the performance measure, it can be seen that WS at 11668 iterations reaches 80% performance (90% at 12773) which for KDE happens just before iteration 633 (90% at 1610). When examining the number of samples still in consideration, WS requires more than 20000 iterations to reduce the number of samples to 2000 which by KDE achieved after just 722 iterations. Both of these observations show that KDE is faster than WS[2].

In previous experiments, the iterative method using KDE was applied to an analytic function used as ground truth. The analytic function describes a PiH case closely related to the one presented in this paper. The result showed that the ten sample points with the highest value estimated by KDE within 1000 iterations were located on a point where the ground truth had a success probability above 99%. This clearly indicates that the presented learning method using KDE is able to find promising regions of parameter space.

Since WS is observed to be five times slower than KDE in the reduction of samples, the WS representation will be omitted in future comparisons.

6.1.2 Comparing KDE Representation and Naïve Sampling

For comparing the KDE regression estimate NS is used. From NS, the normal binomial mean and confidence interval is calculated for each sample point and used as an estimate on the true value. Each point is sampled 100 times which results in a total of 402500 simulation runs.

In Figure 5 two cross-sectional views of the regression value at φ equal $0.0°$ and $11.25°$ for both KDE (left column) and NS (right column) are shown. These two views are highlighted since only approach angles (φ) below $20°$ are usable in real world due to

[2]We do in the comparisons not consider the 5000 samples used for finding the optimal kernel size by Cross-Validation (CV). A suitable kernel size can be chosen from knowledge obtained in previous similar cases.

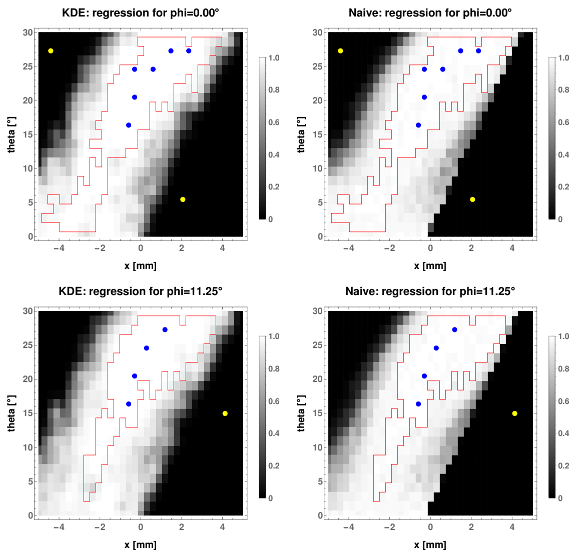

Figure 5: Comparison of the success probability between the KDE and NS results. Each of the four plots represents a cross-sectional view of the parameters x and θ at a fixed φ. The red and blue dots represent the best sample points found by NA and KDE respectively. The yellow dots represent three bad points used for the real world experiment. See text for more information.

accessibility.

By visual inspection, similarities between NS and KDE are clearly seen. Please note that NS is not the ground truth, since only 100 experiments are made in each sample point. However, NS makes for a good comparison since the points are not influenced by smoothing as for KDE.

We compare KDE and NS by finding the best sample points from KDE and by outlining the 99% contour line from NS. However, to avoid selecting close lying points from the KDE result, sample points within a certain region of the already selected sample are rejected. In this case, the choice is made to omit sample points within 2 points of an already selected point for x and θ which corresponds to $0.7\,mm$ and $3.4°$ respectively. The angle φ is not constrained, since this parameter is discretised in steps of $11.25°$. Moreover, to avoid border effects also the samples at x equal $-5\,mm$ and $5\,mm$ and at θ equal $0°$ and $30°$ are eliminated.

In Figure 5 the best points from KDE and the outline of the NS 99% contour line within the two cross-sectional views are shown. The red line represents the NS 99% contour line. Note that 300 of the 318 points within the two 99% contour outline areas have a success probability at 99% or above. The remaining 18 points has at least a success probability at 95%. Moreover, 16 points with a success probability at 99% or above are located outside the contour area due to their

Table 1: Performance of the ten candidate points found.

Sample	Success probability		
number	KDE [%]	Naïve [%]	Re-sam. [%]
1	100.0	100 ± 0.0	98.8 ± 1.0
2	100.0	100 ± 0.0	98.8 ± 1.0
3	100.0	99 ± 2.0	98.4 ± 1.1
4	100.0	100 ± 0.0	98.8 ± 1.0
5	100.0	100 ± 0.0	98.8 ± 1.0
6	100.0	100 ± 0.0	98.8 ± 1.0
7	100.0	99 ± 2.0	98.6 ± 1.0
8	100.0	100 ± 0.0	98.8 ± 1.0
9	100.0	99 ± 2.0	98.2 ± 1.2
10	100.0	100 ± 0.0	97.0 ± 1.5

sparse appearance. The blue dots represents the ten best points chosen by KDE while omitting close lying points.

Figure 5 shows that the ten candidate points suggested by KDE all lies with the 99% contour area from NS. Moreover, these points are mostly located in the middle of the contour area. Seven of the ten points are located on points from the NS point with 100% success probability, while the remaining three points are located on a NS point with a 99% success probability. This clearly indicates that KDE has found a true good region, and that KDE suggests the points pushed away from bad regions and into the middle of a success region even if a plateau appears as for this case.

All ten sample points chosen from KDE results have an estimated KDE regression value above 99.99%. A comparison of these values with the values obtained from NS are shown in Table 1.

6.1.3 Refining the Promising Parameter Sets

Before real world experiments can be carried out, one parameter set needs to be selected. However, just selecting the sample point with the highest regression value among the ten candidates suggested by the iterative learning method might not be the best choice. The regression values obtained by the iterative learning method with KDE are influenced by the kernel smoothing, and do therefore not reveal the true value.

A simple way to deal with this problem is to further test the candidate points by simulations to reveal a more reliable estimate on the true regression value. Each of the ten candidate points is re-sampled 500 times with perturbations, from which the binomial mean and confidence interval have been calculated (see the "Re-sam." column in Table 1). This further testing of these good candidates is only possible due to the reduction of sample points, and would have been infeasible to make for all sample points.

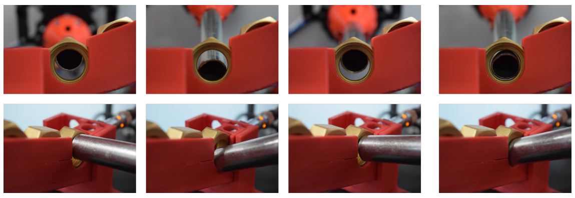
Figure 6: *From left to right:* Three "bad" sample points and the selected "good" point from two different angles. For the "bad" points the peg either collides with the brass fitting below or above the hole and does therefore fail. The images in the right column show a success for the "good" point.

Even though each point in the re-sampling was sampled 500 times, it is impossible to distinguish the ten points by statistical certainty. Moreover, the comparison between the NS and the re-sampling clearly shows that only taking 100 samples in each point are not enough for result to be reliable. This fact just stresses the need for a fast reduction of the parameter space.

The re-sampling shows that six of the ten candidate points all have obtained the highest success probability at 98.8%, and therefore sample number five is randomly chosen for the test on the real world setup.

6.2 Real World Results

In this section real world experiments are carried out based on the results from the previous section. The simulator is rather conservative compared to the real world by not implementing compliance between gripper and pipe, which may be enough to raise the success probability sufficiently.

Besides executing the selected "best" sample point 100 times also several "bad" sample points are tested. These points were chosen manually to show that the promising region found by the iterative learning method in simulation also aligns with the real world case. These "bad" points are shown in yellow in Figure 5.

The three "bad" samples points were tried out once each. As Figure 6 shows these sample points fail to succeed since the peg collides with the brass fitting either below or above the hole. The figure also shows that the "good" sample point selected for execution succeeds. Recall that the approach angle is either 0° or 11.25° for all four points.

After this observation the selected "best" sample point found by the iterative learning method using KDE was tested. The experiments were made by circulating between ten different pipes and brass fittings to introduce part variations. The real world test of the selected "best" sample point was carried out 100 times with a success rate of 100%. The number 100 was chosen as sufficient to show that good parameter sets can be chosen from simulation and executed in real world. A longer test should be conducted to verify that the selected set of parameters is robust to small changes occurring over the lifetime of the setup.

7 SUMMARY

In this paper we proposed an iterative learning method which differs from other methods by being able to take into account part variations and process uncertainty. This property is very important to find action parameters which are guaranteed to succeed every time in precision demanding assemblies as for the Peg-in-Hole task discussed in this paper.

Experiments showed that our iterative learning method is able to quickly reduce of the parameter space using Kernel Density Estimation which takes the neighbourhood region into account. This approach was faster than both neighbourhood independent representation Wilson Score and simple Naïve Sampling. It was shown that KDE is able to find good sample points much faster than a representation which individually estimates the success probability of each of the sample points.

In the conducted experiment, promising sets of parameters were found by the iterative learning method using KDE through simulation. From the knowledge obtained by the method a promising sample point was selected for a real world Peg-in-Hole experiment. The experiment was repeated 100 times with a success rate of 100%. Moreover, real world experiments also showed that the iterative learning method converged successfully towards the promising region of the parameter space.

Future work will study the effect of different bandwidth matrices which might speed up the iterative learning method and potentially improve the quality of the points found. The result when applying the iterative learning method with KDE showed both an over- and underestimation of the regression values in certain spots. These peak spots are probably an effect of a too narrow kernel. An adaptive kernel size should also be investigated since the bandwidth matrix is known to change with the number of samples.

ACKNOWLEDGEMENTS

This work was supported by The Danish Council for Strategic Research through the CARMEN project.

REFERENCES

Agresti, A. and Coull, B. A. (1998). Approximate Is Better than "Exact" for Interval Estimation of Binomial Proportions. *The American Statistician*, 52(2):119–126.

Auer, P., Cesa-Bianchi, N., and Fischer, P. (2002). Finite-time analysis of the multiarmed bandit problem. *Mach. Learn.*, 47(2-3):235–256.

Bodenhagen, L., Fugl, A., Jordt, A., Willatzen, M., Andersen, K., Olsen, M., Koch, R., Petersen, H., and Kruger, N. (2014). An adaptable robot vision system performing manipulation actions with flexible objects. *Automation Science and Engineering, IEEE Transactions on*, 11(3):749–765.

Brochu, E., Cora, V. M., and de Freitas, N. (2010). A tutorial on bayesian optimization of expensive cost functions, with application to active user modeling and hierarchical reinforcement learning. *CoRR*, abs/1012.2599.

Buch, J., Laursen, J., Sørensen, L., Ellekilde, L.-P., Kraft, D., Schultz, U., and Petersen, H. (2014). Applying simulation and a domain-specific language for an adaptive action library. In *Simulation, Modeling, and Programming for Autonomous Robots*, pages 86–97. Springer International Publishing.

Deisenroth, M. P., Neumann, G., and Peters, J. (2011). A survey on policy search for robotics. *Foundations and Trends in Robotics*, 2(1–2):1–142.

Detry, R., Kraft, D., Kroemer, O., Bodenhagen, L., Peters, J., Krüger, N., and Piater, J. (2011). Learning grasp affordance densities. *Paladyn*, 2(1):1–17.

EU Robotics aisbl (2014). Robotics 2020 multi-annual roadmap for robotics in europe.

Even-Dar, E., Mannor, S., and Mansour, Y. (2006). Action elimination and stopping conditions for the multi-armed bandit and reinforcement learning problems. *The Journal of Machine Learning Research*, 7:1079–1105.

Gams, A., Petric, T., Nemec, B., and Ude, A. (2014). Learning and adaptation of periodic motion primitives based on force feedback and human coaching interaction. In *Humanoid Robots (Humanoids), 2014 14th IEEE-RAS International Conference on*, pages 166–171.

Härdle, W., Werwatz, A., Müller, M., and Sperlich, S. (2004). *Nonparametric and semiparametric models*. Springer Berlin Heidelberg.

Heidrich-Meisner, V. and Igel, C. (2009). Hoeffding and bernstein races for selecting policies in evolutionary direct policy search. In *Proceedings of the 26th Annual International Conference on Machine Learning*, ICML '09, pages 401–408. ACM.

Ijspeert, A. J., Nakanishi, J., Hoffmann, H., Pastor, P., and Schaal, S. (2012). Dynamical movement primitives: Learning attractor models for motor behaviors. *Neural Computation*, 25(2):328–373.

Jørgensen, T. B., Debrabant, K., and Krüger, N. (2016). Robust optimizing of robotic pick and place operations for deformable objects through simulation. In *Robotics and Automation (ICRA), 2016 IEEE International Conference on*. (accepted).

Li, B., Chen, H., and Jin, T. (2014). Industrial robotic assembly process modeling using support vector regression. In *Intelligent Robots and Systems (IROS 2014), 2014 IEEE/RSJ International Conference on*, pages 4334–4339.

Park, D., Kapusta, A., Kim, Y. K., Rehg, J., and Kemp, C. (2014). Learning to reach into the unknown: Selecting initial conditions when reaching in clutter. In *Intelligent Robots and Systems (IROS 2014), 2014 IEEE/RSJ International Conference on*, pages 630–637.

Robotics VO (2013). A roadmap for U.S. robotics from internet to robotics.

Ross, S. M. (2009). *Introduction to Probability and Statistics for Engineers and Scientists*. Acedemic Press, 4th edition.

Silverman, B. W. (1986). *Density estimation for statistics and data analysis*, volume 26. Chapman & Hall/CRC press.

Sutton, R. S. and Barto, A. G. (1998). *Reinforcement learning: An introduction*, volume 28. MIT press.

Tesch, M., Schneider, J. G., and Choset, H. (2013). Expensive function optimization with stochastic binary outcomes. In *Proceedings of the 30th International Conference on Machine Learning, ICML 2013, Atlanta, GA, USA, 16-21 June 2013*, pages 1283–1291.

Thulesen, T. N. and Petersen, H. G. (2016). RobWork-PhysicsEngine: A new dynamic simulation engine for manipulation actions. In *Robotics and Automation (ICRA), 2016 IEEE International Conference on*. (accepted).

Williams, R. J. (1992). Simple statistical gradient-following algorithms for connectionist reinforcement learning. *Machine Learning*, 8(3):229–256.

Yang, Y., Lin, L., Song, Y., Nemec, B., Ude, A., Buch, A., Krüger, N., and Savarimuthu, T. (2015). *Fast programming of peg-in-hole actions by human demonstration*, pages 990–995. IEEE.